Co-thermal Degradation Characteristics of Rice Straw and Sewage Sludge

Thi Ngoc Lan Thao Ngo
National Central University

Kung-Yuh Chiang (kychiang@ncu.edu.tw)
Graduate Institute of Environmental Engineering, National Central University, Tao-Yuan City, 32001, Taiwan.

Research

Keywords: Rice straw, Sewage sludge, kinetic analysis, TGA-FTIR, pyrolysis, gasification

Posted Date: January 6th, 2021

DOI: https://doi.org/10.21203/rs.3.rs-139425/v1

Co-thermal degradation characteristics of rice straw and sewage sludge

Thi Ngoc Lan Thao Ngo [1], Kung-Yuh Chiang[1*]

[1] Graduate Institute of Environmental Engineering, National Central University, Tao-Yuan City, 32001, Taiwan.

*Corresponding author

Kung-Yuh Chiang

Ph.D., Professor

Email: kychiang@ncu.edu.tw

Graduate Institute of Environmental Engineering, National Central University, Tao-Yuan City, 32001, Taiwan.

ABSTRACT

This study investigates the kinetic behaviors and gas evolution of rice straw, sewage sludge, and their blends under co-thermal decomposition processes using Thermogravimetric analysis combined with Fourier-Transform Infrared Spectroscopy (TGA-FTIR). The experimental results indicate that sewage sludge could be enhanced the volatile matter decomposition in rice straw co-thermal process at lower temperatures. Activation energy decreases from 53.07 kJ/mol to 48.62 kJ/mol with an increase in sewage sludge addition from 50% to 80% under pyrolysis conditions. The major volatile components were aliphatic chains with double bonds, as well as carbonyl, hydroxyl, and C–H groups in organic compounds by FTIR identification. The tested materials characteristics in terms of volatile matter-to-fixed carbon (VM/FC) ratio was significantly affected the thermal degradation performance. Activation energy was decreased with increasing the VM/FC ratio. It implied that co-thermal reaction could be accelerated. In summary, the results could provide the important information for co-thermal treatment of sewage sludge and rice straw in commercial-scale plant.

Keywords: Rice straw; Sewage sludge; kinetic analysis; TGA-FTIR; pyrolysis; gasification.

Highlights

- Kinetic characteristics in co-thermal treatment of rice straw and sewage sludge was investigated.
- Biomass containing higher volatile matter content has a higher activation energy.
- Blending 40% rice straw and 60% sewage sludge was optimum ratio for co-pyrolysis.
-
- Kinetic results provide the information for the design and operation work in thermal process.

1. Introduction

Approximately 130 thousand tons (based on 80% moisture content) of sewage sludge (SS) derived from municipal wastewater treatment plants (WWTPs) are generated in Taiwan per year. The amount of sewage sludge is expected to dramatically increase due to the rapid increase in sewer system establishment and stringent requirements for water resources protection. Sanitary landfills are currently a major solution for sewage sludge final disposal. Rice production is one of the most important agricultural activities in Taiwan. The average rice straw (RS) generation is nearly 1.5 million tons per year [1]. The common traditional habits of farmers include open firing rice straw treatment. However, this option will not be sustainable at current or projected levels due to increasing competition for landfill space, higher costs, more stringent environmental standards, and the implementation of policies to promote recycling. Energy recovery from rice straw and/or sewage sludge has become an attractive solution using thermal chemical conversion processes including combustion, torrefaction, pyrolysis, and gasification. One of the issues of public concern for energy conversion is sewage sludge containing high moisture content resulting in relatively low energy yield. Sewage sludge and other kinds of organic wastes could be an alternatives technology for solving the obstacles and improving the energy yield. To cope with the increasingly stringent regulations, constantly rising treatment, and final disposal costs of sewage sludge and rice straw, the Taiwan government planned to establish strategies and develop innovative technologies for treating the above wastes and achieving the circular economy target. Among the thermal conversion technologies, gasification is an innovative technology because it has several potential advantages associated with high carbon conversion, high calorific value synthesis gas, and flexible biomass utilization and/or agricultural waste-to-energy [2-5]. On the other hand, sewage sludge and biomass (pine sawdust) co-gasification were also investigated in previous literature [6]. The literature results indicated that co-gasification could improve volatile matter thermal behavior and enhance energy conversion efficiency.

Thermogravimetric analysis (TGA) has become a common analysis technique to investigate thermal behaviour and kinetics. This involves the weight loss characterization of tested materials as a function of the reaction temperature controlled in simulated thermal reaction atmospheres. Typical TGA advantages are accurate real-time sample mass measurements, high reproducibility, and well-defined temperature and gas-phase conditions [7-9]. TGA has been applied in recent years to the study of sewage sludge, rice straw, woody biomass, plastics, and other organic waste thermal characteristics using simulated pyrolysis conditions [6, 10-13]. TGA is coupled with spectrometers, such as Fourier transform infrared spectroscopy (FTIR), to analyze the temporal resolution of specific gas-phase fragments. This contributes to the analysis and understanding of thermal degradation mechanisms before waste and/or biomass treatment [14-17].

However, little information has been collected on the relationships between waste and/or biomass characteristics, reaction kinetics, and gaseous speciation during the thermal degradation process. Moreover, biomass properties play important roles in thermal degradation process determination. Some parameters such as volatile matter (VM), fixed carbon (FC), moisture (H_2O), or elemental contents (C, H, N, S) are key factors that affect the energy conversion process. The volatile and fixed carbon contents in biomass are practical parameters for evaluating the volatility and ignitability [18]. Practically, the different characteristics of biomass fuels from coal to plastic, include their higher volatile matter and lower carbon content. Pyrolysis and gasification system modifications need to consider these characteristics along with other factors carefully. Therefore, the objectives of this research were: (1) to determine the kinetic triplets in co-thermal degradation of rice straw, sewage sludge, and their blends; (2) to understand the characteristics of gas evolution and possible speciation during the co-thermal degardation process; (3) to investigate the relationship between the tested materials characteristics and kinetic triplets during the co-thermal degradation process.

2. Materials and methods

2.1 Materials

The feedstocks used for the co-thermal process in this research were sewage sludge and rice straw, respectively. Sewage sludge was sampled from Dihua urban WWTP, which was established in July 1980 with a capacity of 500,000 m^3/day in Taipei City, Taiwan. Sewage sludge was treated using gravity thickening, anaerobic digestion, and dewatering. To reduce the sludge volume and save transportation cost, sewage sludge dewatered by drying prior to the final disposal. Rice straw was collected from Chung-Li District, Tao-Yuan city located in the northern part of Taiwan. Rice straw and sewage sludge were first dried, shredded, and sieved to extract a particle size between 150 μm and 210 μm. In order to precisely analyze the thermal reaction, rice straw was pelletized using a mini-pellet press due to its light and bulky properties. Proximate analysis indicated the percentage by weight of moisture, ash content, volatile matter, and fixed carbon. The tested samples were determined in triplicate using regulation testing procedures announced by the Taiwan Environmental Protection Administration (EPA) and the Chinese National Standard (CNS) which are similar to the American Standard for Testing Materials (ASTM). The ultimate analysis of the combustibles in the sewage sludge and rice straw was also analyzed in triplicate using an elemental analyzer (Elementar Analyzer Vario MICRO cube). The sewage sludge and rice straw energy contents were determined using a bomb calorimeter (Parr 1341 calorimeter).

2.2 Experimental conditions

Thermogravimetric (TG) analysis is a common technique used to understand thermal behavior and investigate the reaction kinetics in rice straw and sewage sludge co-pyrolysis and/or gasification. The thermogravimetric analyzer (TGA) used in this study is a commercially available laboratory instrument (TGA-STA 7300, Thermal Analysis System, Hitachi). The dried

sewage sludge was prepared by drying and mixing with 20 wt.%, 40 wt.%, and 50 wt.% of rice straw, respectively. The TGA experiments were performed from 40 °C to 1000 °C and operated at heating rates of 5, 10, 20 °C/min in different pyrolysis and /or gasification atmospheres. In the pyrolysis experiments, about 3 mg of the tested samples were pyrolyzed under 100 ml/min with 100% N_2 as the carrier gas. To further simulate the gasification atmosphere air and nitrogen was well-mixed as the carrier gas and controlled between 0.3 vol.% and 1.0 vol.% air mixing ratio under total a flow rate of 100 ml/min.

Rice straw and their blends were evaluated using TGA and TGA-FTIR (Fourier Transformer IR) analysis. To determine the thermal reaction conditions, raw materials were placed in a ceramic crucible 5 mm in inner diameter and 5 mm in height. A precision balance constantly weighed the crucible carrying the samples with a resolution of 0.1 µg. At different reaction rates (5, 10, 20 °C/min), the total time needed for the entire process was calculated. A change in the heating rates brings a corresponding change in air/N_2 ratios of 0.3/99.7, 0.5/99.5, and 1.0/99.0, respectively. Figure 1 illustrates the schematic diagram of an experimental set-up for TGA-FTIR.

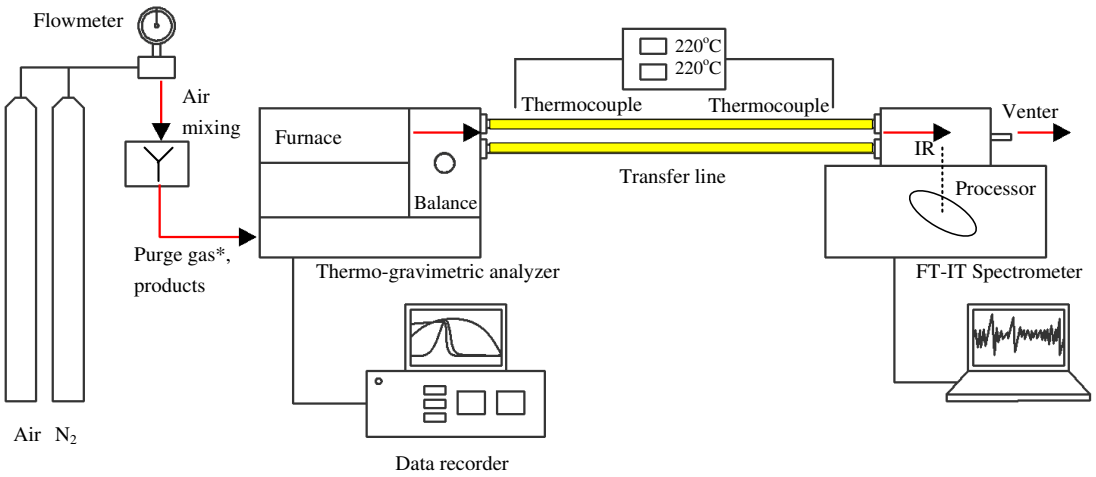

Note the purge gas* used were nitrogen and air for TGA and TGA-FTIR, respectively.

Figure 1. Schematic diagram of TGA-FTIR experiment

136

137

138 **2.3 Kinetic analysis**

139 The thermal decomposition reaction kinetics of carbonaceous materials is complicated. The
140 kinetic parameters were determined, including activation energy, reaction order, and pre-
141 exponential factor, respectively. The activation energy was determined using the integral method
142 [5, 19] that can be simply expressed as the Arrhenius equation:

143 $$\frac{dX}{dT} = - Ae^{-(\frac{E}{RT})}X^n \qquad (2)$$

144 Where

145 A: pre-exponential or frequency factor (min^{-1});

146 E: decomposition reaction activation energy (kJ/mol);

147 n: order of reaction;

148 R: universal gas constant (kJ/mol.K);

149 t: time (min); T: absolute temperature (K).

150 The multiple linearized regression form of the Arrhenius equation was used to determine A,
151 E, and n by applying a least-squares (multiple linear regression) techniques. The ideas for
152 calculating reaction order were introduced by previous published literature [20]. Multiple
153 regression analysis can be regarded as an extension of straight-line regression to the situation in
154 which more than one independent variable must be considered. The implied form of the
155 linearized rate equation is

156 $$y = B + Cx + Dz \qquad (3)$$

157 The parameters y, x, z B, C, and D in Eq. (3) are defined as follows

158 $$y = \ln\left\{\left[\frac{-1}{(w_o - w_f)}\right]\left(\frac{dw}{dt}\right)\right\} \qquad (4)$$

159 $$x = \frac{1}{RT} \qquad (5)$$

$$z = \ln\left\{\frac{(w - w_f)}{(w_o - w_f)}\right\} \quad (6)$$

Where w: weight of sample at time t (min); w_f: weight of residue at the end of the reaction (g); w_o: initial weight of the sample. The coefficients B, C, and D in Eq. (2), which correspond to the logarithm of the pre-exponential factor ln A; the activation energy E; and the reaction order n, respectively, were determined for each type of rice straw, sewage sludge and their mixture using the multiple linear regression analysis methods using thermo-gravimetric data by Statistica software (Data analysis-software system, version 10).

3. Results and discussion

3.1 Analysis results of thermal kinetic

3.1.1 Comparison between the pyrolysis and gasification of rice straw

The physical-chemical characteristics of rice straw and sewage sludge are shown in Table 1. Elemental analysis shows that tested samples have high carbon content at nearly 40%. The higher heating value of sewage sludge (4,200 kcal/kg) was higher than that of rice straw (3,800 kcal/kg). The higher heating value of these materials has proven that sewage sludge and rice straw have potential as bio-fuel for themal processes. Nevertheless, volatile matters, which are the key factor in thermal conversion process improvement on average at 59.38% and 64.22% from sewage sludge and rice straw, respectively.

Table 1 Characteristic of tested sewage sludge and rice straw

	Sewage sludge	Rice straw
Proximate analysis (wt. %)		
Moisture	6.71 ± 0.88	10.47 ± 0.97
Ash	23.02 ± 0.12	9.56 ± 0.22
VM	59.38 ± 0.16	64.22 ± 0.47
FC	10.89	15.75
Ultimate analysis (wt. %, dry basis)		
C	39.74 ± 0.91	39.86 ± 0.59
H	5.89 ± 0.15	6.18 ± 0.18
N	6.5 ± 0.17	0.94 ± 0.05
S	1.14 ± 0.05	0.23 ± 0.05
O	17.0	32.76

Energy content (kcal/kg)		
HHV	4,200 ± 20	3,800 ± 60
LHV	3,500	2,900

Figure 2 shows thermogravimetric analysis TG (in wt.%) and derived thermogravimetric DTG (in wt.%/min) curves obtained during the decomposition of rice straw in pyrolysis and gasification at heating rates of 10 ºC/min from 40 ºC to 1000 ºC. From the DTG curves, it could be illustrated that only one peak is observed in the DTA graph corresponding to the number of degradation stages. Besides, the temperature of the peak in the DTA corresponds to the temperature at which max degradation occurs. As observed in Figure 2, the pyrolysis process can be divided into three main stages. At the first stage (40-178 ºC) corresponds to the moisture lost during drying, about 1.71 wt.% of rice straw. The second step (179-500 ºC) relates to organic matter decomposition, and about 57.75 wt.% of the biomass was lost during this stage. The final stage (>500 ºC) is inorganic matter degradation (residual). The sample weight loss during rice straw pyrolysis was 71.51 wt.%. The weight decreased rapidly, attributed mainly to cellulose, hemicellulose, and partial lignin devolatilization [21-22]. The lignin decomposition continued to give a gradual weight loss beyond 450 ºC. Hemicellulose and cellulose pyrolysis occurred rapidly in the range of 250–340 ºC and 340–400 ºC, respectively, contributing to a sharp drop in the TG profile [23].

In a partial oxidative atmosphere (gasification process), rice straw thermal degradation can be classified into three steps, (i) moisture evaporation, (ii) cellulose, and hemicellulose pyrolytic decomposition and (iii) lignin and char oxidative pyrolytic decomposition. The first step was from room temperature to 175 ºC, with about 3.38 wt.% rice straw weight. The second step is the fast decomposition stage, from 176 ºC to 530 ºC. About 55.9% of the weight is lost during this stage. During the whole gasification process, weight loss is about 70.51%. The rice straw weight loss performance was similar under both pyrolysis and gasification conditions at low temperatures, showing that the presence of an air atmosphere did not contribute to the increasing sample decomposition rate.

3.1.2 Effect of added sewage sludge on thermal performances

As seen in Figure 2, a comparison between the pyrolysis/gasification behavior of sewage sludge and rice straw blends can also be made. According to the results, the weight loss profiles for rice straw, sewage sludge, and additives obtained from pyrolysis slightly differ from that of gasification. Thermal degradation of both RS, SS and their additives during pyrolysis in an inert atmosphere can be classified into three main stages including (i) moisture evaporation, (ii) main devolatilization, and (iii) continuous devolatilization. The beginning and ending temperatures of the decomposition process are important characteristic parameters for feedstocks. In the case of pyrolysis, the beginning sewage sludge and rice straw temperatures were 153 ^{o}C and 178 ^{o}C, and the corresponding ending temperatures were 517 ^{o}C and 500 ^{o}C, respectively. Sewage sludge and their blends, the major decomposition temperature at a lower temperature range varies 147-173 ^{o}C to 515-535 ^{o}C. The final weight loss at the end is close to 500 ^{o}C due to ash and fixed carbon, which are not decomposed at this temperature. Rice straw and sewage sludge have narrow decomposition temperature ranges for adding rice straw samples resulting in T_i decreasing by 5-31 ^{o}C. This indicates that adding sewage sludge to rice straw results in shifting to lower initial decomposition temperature compared to that of rice straw. Comparing with the pyrolysis process, DTG gasification performance curves also show one prominent reaction zone exists in the heating rate range studied and the SS, RS weight loss and their blends have the same trends (Figure 2b). The weight loss curve results for the tested samples are recognized to have similar trends, meaning that these materials have potentially promising applications in co-pyrolysis/gasification. This proved that biomass and their blends have the same pyrolysis and gasification thermal decomposition behavior and the thermal degradation of all materials occurred in a single stage.

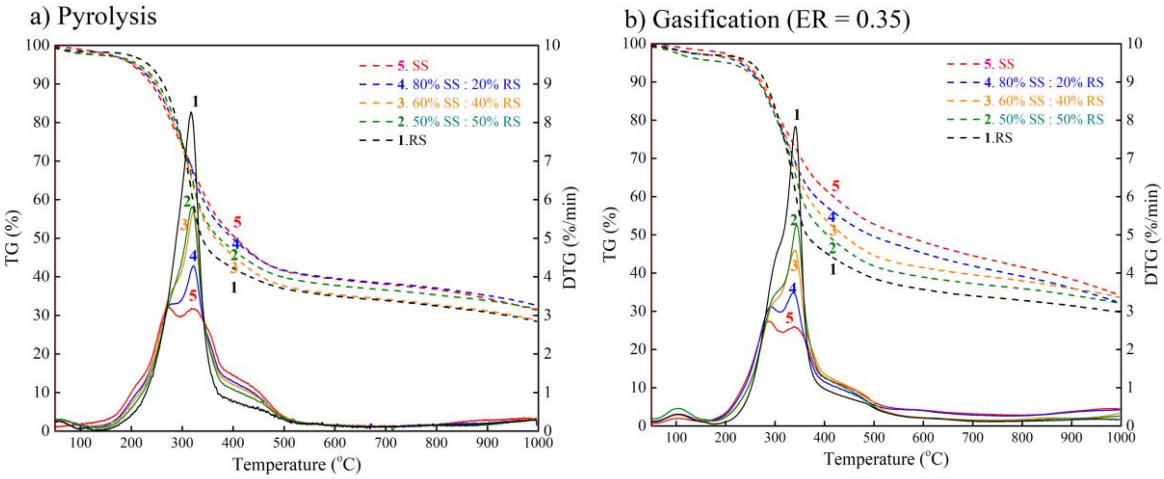

225

226 **Figure 2**. A comparison between TG/DTG curves detected from rice straw, sewage sludge and
227 their additives pyrolysis and air gasification at 10 °C/min heating rate
228

229 Table 2 shows some kinetic parameters (activation energy and pre-exponential factor) and
230 temperature range (TR) of rice straw, sewage sludge, and blends thermal decomposition
231 behavior obtained from pyrolysis and gasification simulations. In rice straw pyrolysis analysis,
232 the activation energy obtained by the Arrhenius plot method was 75.40 kJ/mol for a heating rate
233 of 10 °C/min. Sewage sludge was observed to react faster during pyrolysis compared to rice
234 straw. The lower activation was found at 49.10 kJ/mol, which may be due to the slightly higher
235 amount of ash in sewage sludge. This conclusion is consistent with the previous published
236 literature result that reduced the activation energy from 87.7 kJ/mol to 51.6 kJ/mol by adding
237 oil-palm solid wastes into paper sludge under pyrolysis conditions [23]. The higher activation
238 energies were obtained for gasification 89.56 and 60.12 kJ/mol in rice straw and sewage sludge,
239 respectively. Rice straw was found to be more reactive to gasification compared to sewage
240 sludge. This is due to the relatively higher amount of volatile matter in rice straw compared to
241 sewage sludge. Highly reactive combustible components may account for the high reactivity
242 towards gasification by sewage sludge samples. As shown in Table 2, the activation energy
243 increases with increasing rice straw addition in the 48.62-53.07 kJ/mol range in pyrolysis and
244 63.73-68.66 kJ/mol under gasification conditions with 20 wt.% to 50 wt.% addition ratio.

In the multiple regression model, the multiple correlation coefficient (r^2) value indicates the dependent variable relation (activation energy) and two other predictor variables (pre-exponential and reaction order). Table 2 shows the coefficient of multiple correlations are in the region of 0.7~0.9 and is not a measure of the straight-line model appropriateness. The linear regression establishing the relationship between the fitted line and all of the activation energy and time function data points, respectively. The strong correlation coefficients have partial correlation (r^2) in the 0.9~0.99 range and decrease slightly by adding one more variable (reaction order). The calculating reaction order idea was introduced in numerous studies [7, 19, 24]. The biomass reaction order was found at around 0.69-3.57 (as indicated in Table 3) [25-39]. The reaction order values were different from stage to stage and changed with different fuel mixing ratios.

The rice straw and their blends exponential factors were in the 0.71×10^5-18.6×10^6 (s^{-1}) pyrolysis condition range. Higher pre-exponential values were found in the gasification simulation, with the higher estimated value in the 1.97×10^5 - 0.59×10^8 (s^{-1}) range, respectively. That can be explained by oxidation reactions occurring after the gasification process, from reaction by-products that include syngas, char and tar productions, respectively. Tar product is decomposed due to the presence of oxygen, making the thermal decomposition process longer than pyrolysis. The results were also confirmed by previous published literature [26, 27]. Similar phenomena occurred in this research with higher activation energy found under gasification conditions due to highly reactive ash components. Comparison of different atmospheres, it leads to the conclusion that an increasing tendency in the increasing degree of oxidation causes the increases in the degradation rates and shifts the decomposition of non-biodegradable matter to lower temperatures, since a more exothermal balance.

Table 2. Kinetic constants for pyrolysis, sample gasification at 10°C/min heating rate

Items	Pyrolysis (N_2 atmosphere)			Gasification (air atmosphere)		
	TR(°C)	Thermal decomposition rate	r^2	TR (°C)	Thermal decomposition rate	r^2
SS	153-517	$k = 1.37 \times 10^5\ e^{49.10/RT}(X)^{2.41}$	0.90	148-550	$k = 1.97 \times 10^5\ e^{60.12/RT}(X)^{3.57}$	0.84
20RS:80SS	173-535	$k = 0.71 \times 10^5\ e^{48.62/RT}(X)^{1.52}$	0.86	154-659	$k = 5.40 \times 10^5\ e^{63.73/RT}(X)^{3.30}$	0.81
40RS:60SS	154-515	$k = 0.84 \times 10^5\ e^{50.61/RT}(X)^{0.9}$	0.84	160	$k = 14.4 \times 10^5\ e^{64.31/RT}(X)^{2.45}$	0.78
50RS:50SS	147-516	$k = 1.44 \times 10^5\ e^{53.07/RT}(X)^{0.69}$	0.83	160-551	$k = 19.1 \times 10^5\ e^{68.66/RT}(X)^{2.26}$	0.80
RS	178-500	$k = 18.6 \times 10^6\ e^{75.40/RT}(X)^{1.43}$	0.82	166-534	$k = 0.59 \times 10^8\ e^{89.56/RT}(X)^{2.12}$	0.71

r^2 in a multiple regression model

3.2 Thermal decomposition kinetics of different types of biomass

Table 3 summarizes some characteristic parameters obtained from pyrolysis/gasification thermogravimetric data. The followings are initial weight loss (T_i), temperature parameters at the end of the reaction (T_f), the corresponding peak temperatures (T_P) of thermal decomposition behavior with different types of biomass such as rice straw, rice husk, sugarcane baggage, pinewood, sewage sludge, etc. via Arrhenius law in the literature [28-39]. Biomass kinetic analysis plays an important role in determining the reaction kinetics necessary for mathematical modeling and reactor operational parameter optimization. TGA analysis of raw materials was therefore considered during the pyrolysis/gasification conditions.

The physical characteristic of the wastes influences the thermal digestion process related to the temperature peak (T_p). In thermal conditions, when these materials are exposed to high temperatures, their structure, and atomic configuration are changed, which causes some exothermic or endothermic peaks to appear in the thermal diagram [40]. When the DTG curves have a peak, it implies that at this temperature, the molecular relaxation becomes greater and promotes the process to a faster reaction rate. Table 3 illustrates the peak temperature for the decomposition process, which occurs mostly in the 270-350 °C range. Higher peak temperatures 358-491 °C were found, particularly in coal and polypropylene. Volatile matter is highly thermal sensitive. High volatile matter content indicates that a large amount of weight will be lost under high temperatures in the thermal digestion process. Maintaining the pyrolysis/gasification temperature below T_{final} (maximum temperature) to avoid significant mass and energy loss must

292 be carefully considered [41]. Furthermore, some wastes are incomplete decomposition
293 conditions in the temperature range near 600 ^{o}C. This may suggest that the pyrolysis temperature
294 must be controlled at lower degrees than 600 ^{o}C in order to ensure the majority of the material
295 reacts and decomposes.

296 In general, material that has low activation energy requires more input energy demand.
297 Therefore, the tested sludge has higher fixed carbon content that it required more energy for the
298 thermal decomposition process. To further understand the enhanced syngas yield tendency in
299 gasification-oxidation reaction ($C + ½ O_2 \rightarrow CO$), the carbon-to-fixed carbon (C/FC) ratio was
300 used as an index for the gasification reaction. The experimental results indicated that the
301 activation energy of the tested sludge samples were ranged from 50 to 100 kJ/mol with C/FC
302 ratio ranged between 2 and 4. It implied that the tested sludge could easily produce more CO
303 which improves the producer gas lower heating value due to carbon partial oxidation reaction
304 progression. The kinetics of co-pyrolysis/gasification were thoroughly investigated by previous
305 published literature [42-47]. The experimental results indicated that biomass could enhance the
306 degradation of plastics corresponded with an increase in light liquid products [45]. Co-pyrolysis
307 of biomass and plastic could promote as well to obtain high quality chars with higher calorific
308 values as compared bio-chars only generated in biomass pyrolysis [46]. The iso-conversion
309 method was developed by previous published research that could calculate the kinetic parameters
310 in co-pyrolysis of microalgae biomass and low-rank coal [47]. Therefore, TGA results could
311 contribute to enhance the knowledge of tested materials containing high C/FC ratio thermal
312 degradation characterization and to establish the optimum operation conditions for syngas
313 production.

314
315
316
317
318
319

Table 3. Comparison of the kinetic analysis in this study and those in the literature using the Arrhenius law with different biomass types.

Feedstocks	Carrier gas	Flow rate (ml/ min)	Ti	T_{p1}	T_f	E (kJ/mol)	A (min^{-1})	n	r^2	Ref.
Rice straw	N_2	100	178	319	500	75.40	18.6×10^6	1.43	0.82	This study
	Air	100	175	323	530	89.56	0.59×10^8	2.12	0.71	
Sewage sludge	N_2	100	153	272, 321	517	49.10	1.37×10^5	2.41	0.90	This study
	Air	100	148	273, 325	550	60.12	1.97×10^5	3.57	0.84	
20%RS+80%SS	N_2	100	173	324	535	48.62	0.71×10^5	1.52	0.86	This study
	Air	100	154	279, 324	659	63.73	5.40×10^5	3.3	0.81	
40%RS+60%SS	N_2	100	154	321	515	50.61	0.84×10^5	0.9	0.84	This study
	Air	100	160	323	551	64.31	14.4×10^5	2.45	0.78	
50%RS+50%SS	N_2	100	147	320	516	53.07	1.44×10^5	0.69	0.83	This study
	Air	100	166	325	534	68.66	19.1×10^5	2.26	0.80	
Rice straw	N_2	100	266	320	353	59.93	2.4×10^4	1.0	0.995	[28]
Sewage sludge		100	248	310	385	19.66	13.91	1.0	0.998	
Sewage sludge	N_2	50	150	299	550	31.87	27.35	1.1	0.982	[29]
Sewage sludge	H_2O–Ar	150	-		-	65.7	3.9×10^3	1.0	0.998	[30]
Industrial sludge		150	227	-	527	68.08	1.07×10^4	1.0	0.991	
Fluff		150	227	-	527	83.0	1.27×10^5	1.0	0.951	
Scrap tire powder		150	227	-	527	132.4	4.1×10^8	1.0	0.994	
Rice husk	N_2	100	172	348	576	87.41	1.32×10^7	-	0.984	[31]
Rice husk	Air (1st zone)	-	191	321	-	53.4	3.77×10^6	1.41	-	[32]
	Air (2nd zone)		321	-	510	20.8	1.41×10^3	0.47		
Sugarcane bagasse	N_2 (1st zone)	20	140	325	-	53.5	0.28	0.4	0.995	[33]
	N_2 (2nd zone)		325	-	493	43.0	0.15	0.3	0.971	
Cotton stalks	N_2 (1st zone)	20	150	287	-	102	1.22	1.0	0.997	
	N_2 (2nd zone)		287	-	471	98.5	0.45	0.7	0.966	
Chlorella vulgaris	Air	25	165	-	367	41	3.9981	-	-	[34]
Pine wood	N_2	45	245	-	405	68.71	1.75×10^2	-	-	[35]
Activated carbon	N_2	45	80	-	800	5.32	6.43×10^{-5}	-	-	
Coal Char	N_2	600	506.5		653.3	130.12 - 153.17	7.12×10^3	1.0	>0.96	[36]
Coal Char	CO_2	200-500	760	-	820	285.46	3.9×10^{11}	-	-	[37]
Coal	Air	50	-	-	-	52.7	3.3×10^9	-	-	[38]
	O_2	50	-	-	-	93.1	1.3×10^{10}	-	-	
Coal	N_2 (1st zone)	30	174	358	-	36.9	378	1.0	0.986	[39]
	N_2 (2nd zone)		358	491	-	128.9	5.5×10^8		0.995	
	N_2 (3rd zone)		491	-	667	115.4	1.8×10^6		0.976	
HDPE	N_2	30	439	-	523	457.2	3.5×10^{30}	1.0	0.998	
LDPE	N_2	30	426	-	526	300.4	2.2×10^{20}	1.0	0.998	
Plastic (PP)	N_2	30	399	491	507	319.7	5.9×10^{21}	1.0	0.998	

- : not available

T_i, T_p and T_f express the initial, peak and final temperature of volatile matter release

R^2: correlation coefficient

3.3 Characterization of the gas evolution during the co-thermal degradation of rice straw and sewage sludge

Figure 3(a) shows the 3D FTIR diagram of the rice straw pyrolysis process with a heating rate of 10 °C/min. The results indicated that four pyrolysis stages occur at the temperature ranges

of 40-178ºC, 179-319 ºC, 320-500 ºC, and above 500 ºC. Figure 3 (b) displays the observed change in the FTIR spectra during the rice straw pyrolysis process. The main gas phases that occur in pyrolysis include CO, CO_2, CH_4, HCl, aldehyde, CH_3COOH, phenol, and methanol. Based on the results obtained from TG-DTG curves (as shown in Figure 2), the results showed the chemical reaction occurs to change from one phase to others, either the endothermic reaction (usually for melting) or exothermic reaction (e.g. crystallization, release some energies). The first stage is related to the dewatering process (moisture content evaporation) from the start of run 40 ºC to 178 ºC. During this stage, the amount of water vapor increases, and the identifiable gaseous product is water. The initial peaks at 1750-1250 cm^{-1} and 4000-3200 cm^{-1} represents of moisture within the biomass and sludge as detailed by the published literature [13, 15, 35, 48, 51]. The second stage corresponds to biomass decarboxylation and oxidation. When the temperature is higher than 151 ºC, the rice straw chemical structure starts to change dramatically. Some gaseous products are detected in this stage, such as CO_2, CO, CH_4, and water vapor. The band at 2920 cm^{-1} represents C-H stretching. The band at 2350, 2250 cm^{-1} is assigned to the carbonyl (C=O) stretching. Carbonyls mainly exist in the side chains of lignin structural units. The band near 3000-2600 cm^{-1} can be described as C-H bending in cellulose and hemicellulose. The peak at 2250-2000 cm^{-1} is indicative of C-O stretching.

The TGA-FTIR spectra for rice straw demonstrate characteristic peaks involved in the representative of SO_2. The literature results reported that the aromatic compounds at the absorbance wavenumber of 1342 cm^{-1} and 1600-1450 cm^{-1} [52]. This suggests that the second stage was mainly responsible for the initial decomposition of rice straw contaminants. When the operation temperature was reached to 500 ºC, almost all functional groups are eliminated due to organic matter decomposition. Gaseous products are now generated, such as H_2O, CH_4, and phenol (C_6H_5OH) that would be further decomposed in the third stage. According to the analysis results of TGA-FTIR, the evolution of gaseous products increases with the temperature, reaching their maximum values between 178 and 500 °C. At the higher temperature range from 500 °C

354 to 1000 °C, the release of pollutant gases is almost negligible due to the pyrolysis reaction
355 completion.

356 TG-FTIR is also a good technique for determining the different gaseous species existing
357 during different thermal decomposition processes. Figure 3 (c) showed the gas evolution in the
358 rice straw gasification. Gasification is a partly oxidizing process that converts biomass into
359 useful energy such as syngas, which contributes to developing hydrogen, methanol, and
360 synthetic fuels [53]. In the air, the gasification process air is injected into the TGA-FTIR. The
361 IR spectra results show that more CO, CO_2 products are measured under the operating condition.
362 That can be explained using the following reactions (R_1-R_3):

363 $$C + ½\ O_2 \rightarrow CO \text{ Carbon partial oxidation} \quad (R_1)$$

364 $$CO + ½\ O_2 \rightarrow CO_2 \text{ Carbon monoxide oxidation} \quad (R_2)$$

365 $$C + O_2 \rightarrow CO_2 \text{ Carbon oxidation} \quad (R_3)$$

366 The major producer gases in rice straw gasification, including CO_2, CO, CH_4, HCl, NO,
367 ether, alcohol, and phenol, were a little bit different with that of producer gases in pyrolysis. The
368 two highest peaks were found at 319 °C and 323 °C corresponding with the FTIR spectrum for
369 volatiles in rice straw gasification. Partial air oxidation reaction could promote the reaction rate.
370 However, a benzene skeleton was found in the pyrolysis case. SO_2 gases were found in
371 gasification due to the sulfur contained in the rice straw and formation under the partial oxidation
372 atmosphere. On the other hand, the higher and broader peak related to organic hydrocarbon
373 compounds, such as C-O stretching at wavenumber as 1300-950 cm^{-1}, was found in rice straw
374 pyrolysis. This could explain that some interactions existed such as hydrogen bonding
375 interaction. Therefore, if the peak is broader, it could mean the number of bonds occurs in the
376 gas product must be considered. More tar (oil) is generated by pyrolysis compared with
377 gasification.

378

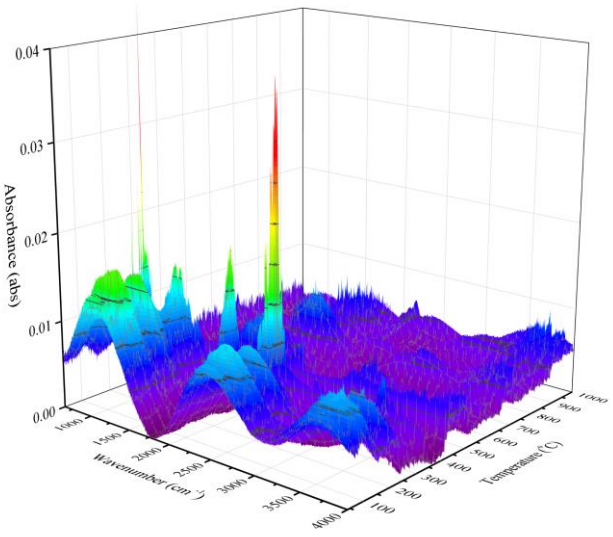

379

380 a) 3D FTIR diagram of rice straw

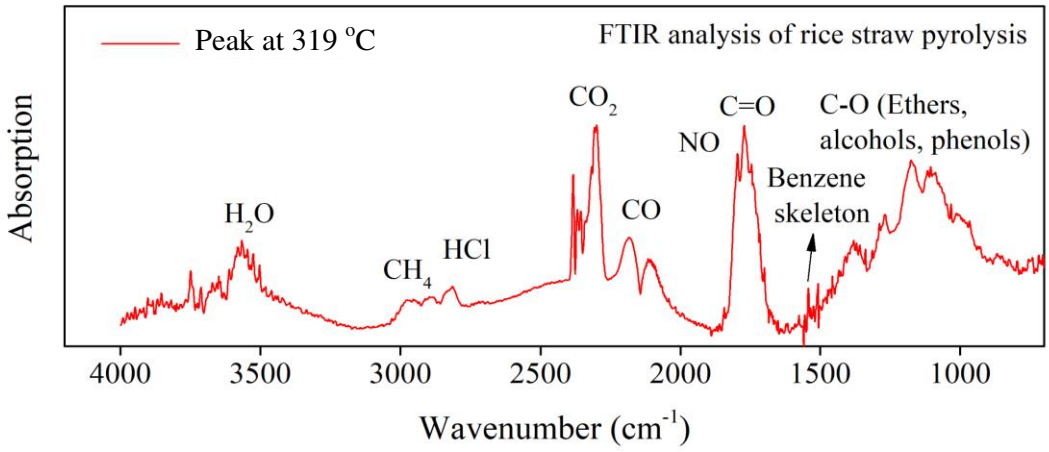

381

382 b) FTIR spectrum for volatiles in rice straw pyrolysis

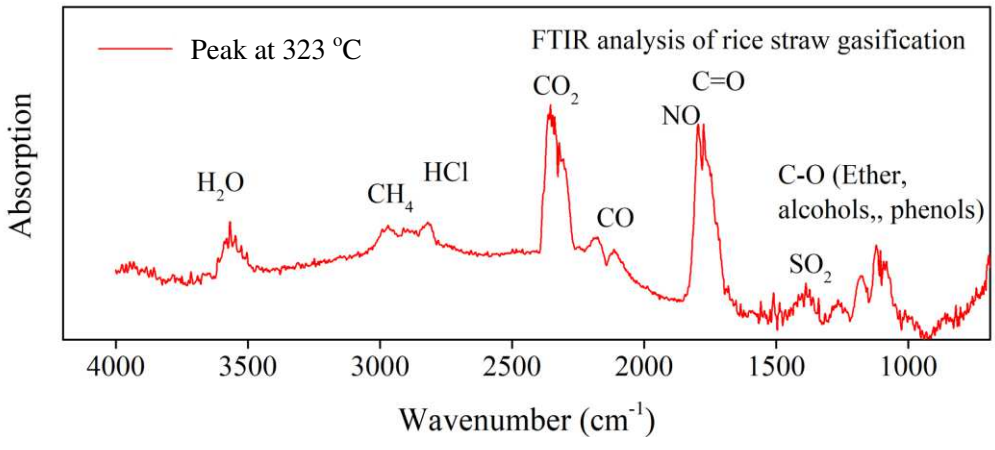

383

384 c) FTIR spectrum for volatiles in rice straw gasification

385 **Figure 3.** FTIR analysis of rice straw pyrolysis/gasification with a heating rate of 10 °C/min

386 The FTIR spectrum indicated the gases generated during rice straw and sewage sludge
387 mixture pyrolysis (rice straw proportion from 0 to 50 % as a function of both wavenumber and
388 temperature. Figure 4 (a) illustrates that the gases evolution of the 3D FTIR diagram in pyrolysis
389 of sewage sludge (0% of rice straw) and mixtures with 20%, 40%, and 50% of rice straw. The
390 main volatile components in organic compounds identified by FTIR were aliphatic chains with
391 double bonds accompanying C=O, OH-, and C–H groups. The major functional groups and
392 gaseous species were measured in the pyrolysis reaction, including C=O stretching (2400-2250
393 cm^{-1}), C-O stretching (2240-2000 cm^{-1}), C-H stretching (3000-2600 cm^{-1}), O-H (4000-3500 cm^{-1}), SO_2 (1350 cm^{-1}), HCl (2789 cm^{-1}), and NH_3 (850-736 cm^{-1}). During the pyrolysis process,
395 specific chemical compounds, such as syngas, aldehyde, acid gas or polluted air (HCl, SO_2, NH_3),
396 were determined by TGA-FTIR. Figure 4 (b) shows the TGA-FTIR spectrograms representing
397 possess characteristic absorption bands within the 1700-800 cm^{-1} region, such as acetic acid,
398 toluene, phenol, and formic acid. With the presence of NH_3, HCl and other acid gases were
399 detected by TGA- FTIR revealing a similar trend that it was confirmed by previous pyrolysis
400 works [49, 54]. Figure 4 (c) illustrates clearly the characteristic infrared absorption peaks of the
401 volatile components. That was observed that absorbance increases with higher gas concentration
402 when the rice straw mixing ratio is increased from 0% to 40%. It implied that increasing the rice
403 straw mixing ratio up to 40% increases the concentration of the gaseous product. However, in
404 the case of the rice straw content increasing from 40% to 50 %, the gaseous products seem to be
405 decreased due to the corresponding with lower absorbance. This is because the hydrocarbon
406 reformation and/or water-gas shift reactions could be inhibited. Besides, ash agglomeration
407 could be occurred and block oxygen diffusion into the char particles due to the rice straw
408 containing a high potassium and silicon concentration [55].
409 Table 4 displays the detected gaseous species adsorption bands during pyrolysis and further
410 presents a comparison between the present study and that of other previous researchers using
411 TG-FTIR [14-16, 35, 48-50]. The waste materials (biomass and sludge) pyrolysis process

412 presents CO_2 CO, CH_4, CH_3COOH, HCOOH, methanol, phenol, and esters as the main gaseous
413 species produced. The rice straw chemical structure was indicated that the abundant chemical
414 bonds were O-H, C-H, C=C and C-O, and aromatic C=C/C-H. It implied that the aromatic
415 compounds formation was probably released by the pyrolysis oils which were determined as
416 aromatic C-H bond bending (wavenumber was between 2000 and 1660 cm^{-1})[51]. The literature
417 results were also proved that some weak peaks were representing aromatic hydrocarbon in the
418 1400-1000 cm^{-1} range [50]. Based on the TG-FTIR analysis results, the main groups in the rice
419 straw were aliphatic chains with double bonds, as well as carbonyl (C=O), hydroxyl (O-H) and
420 alkane (C-H) and alkyl amine. In summary, the experimental results suggested that rice straw
421 controlled at the mixing ratio of 40 wt.% with 60 wt.% sewage sludge could be the optimum
422 conditions in co-thermal treatment. From the kinetic analysis results, rice straw and sewage
423 sludge co-gasification can reduce the required activation energy and enhance the reaction rate.
424 This study discussed how mixing rice straw with sewage sludge could simulate the pyrolysis and
425 gasification process and quantitatively analyze the gaseous components. Further studies are
426 necessary to understand the FTIR that gives reliable quantitative information regarding the
427 functional groups presented.

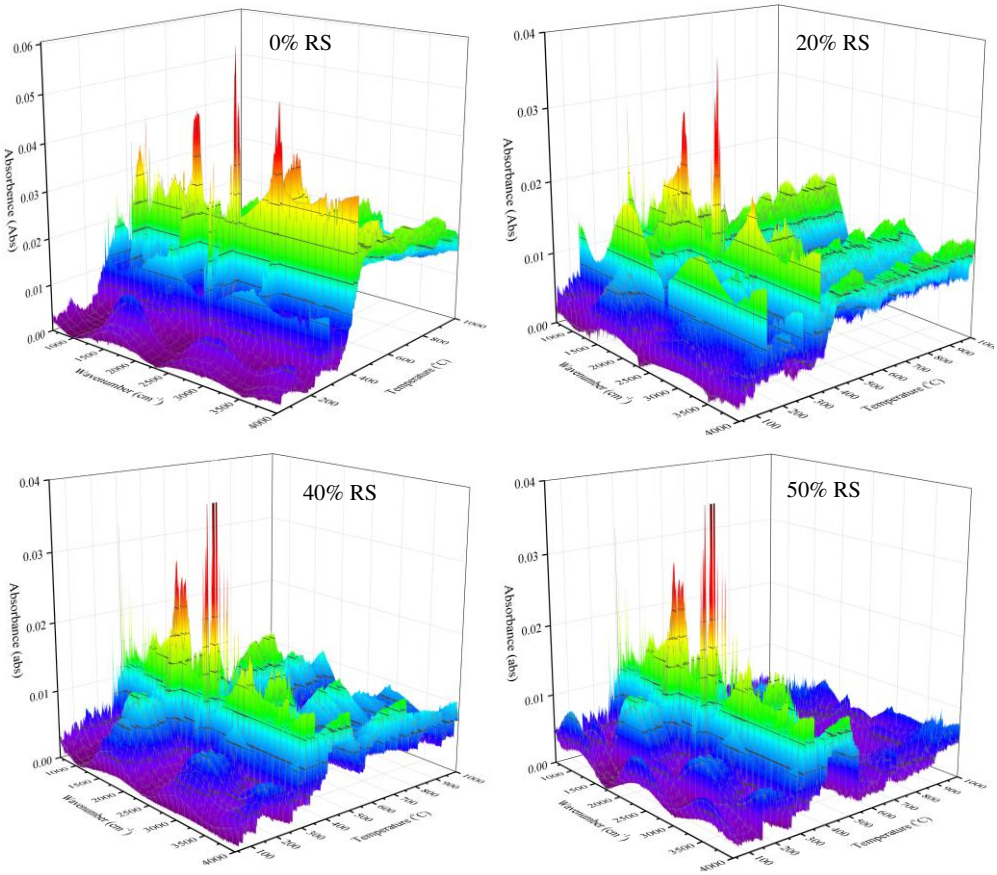

a) 3D FTIR diagrams

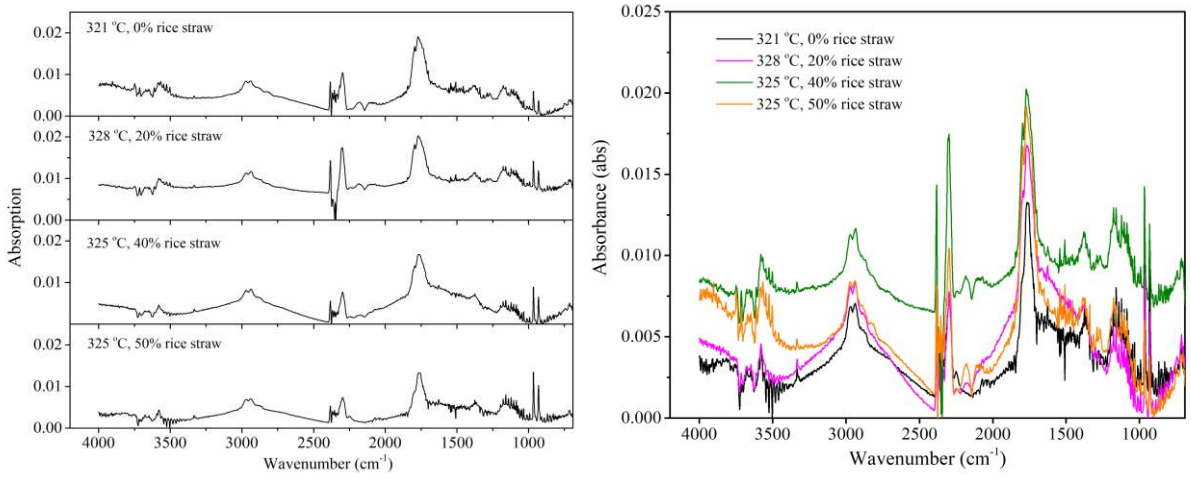

b) FTIR absorption spectra of products evolved during co-pyrolysis.

Figure 4. Gas released from sewage sludge, and their mixtures with rice straw as detected by TGA-FTIR

434 **Table 4.** Gaseous species based on wavenumbers (cm^{-1}) and functional groups for pyrolysis studies

Sample	Wavenumber range (cm^{-1})	Peak (cm^{-1})	Species	Functional group	Vibration	Ref.
Rice straw, sewage sludge, and their blend	2375 - 2250	2350, 2250				This study
Wood, plastic, tire, and RDF	2400 - 2250	2350				[14]
Spruce and pine biomass	2400 - 2240	2359, 2322				[35]
Straw with absorbed glycerol	2400 - 2240	2360	CO_2	C=O	Stretching	[48]
Solid waste, paper mill sludge, and their blends	2400 - 2240					[49]
Marine sediment	2400 - 2240					[16]
Palm kernel shell (PKS) from palm oil	2400 - 2250					[50]
Rice straw, sewage sludge, and their blend	2167 - 2120	2170				This study
Wood, plastic, tire, and RDF	2250 - 2000	2110, 2200				[14]
Coals, sawdust, rice straw, and corn stalk	2240 - 2027		CO	C-O	Stretching	[15]
Palm kernel shell (PKS) from palm oil	2250 - 2000					[50]
Solid waste, paper mill sludge, and their blends		2178				[49]
Marine sediment	2240 - 2060					[16]
Rice straw, sewage sludge, and their blend	3000 - 2600	2920				This study
Wood, plastic, tire, and RDF		2930				[14]
Spruce and pine biomass	3000 - 2600	2897, 2821				[35]
Coals, sawdust, rice straw, and corn stalk	3045 - 2875		CH_4	C-H	Stretching	[15]
Palm kernel shell (PKS) from palm oil	3000 - 2700					[50]
Straw with absorbed glycerol		3100				[48]
Solid waste, paper mill sludge, and their blends	3100 - 2850	3016				[49]
Marine sediment	3000 - 2880					[16]
Rice straw, sewage sludge, and their blend	3964 - 3500	3800, 3600				This study
Wood, plastic, tire, and RDF	4000 - 3500					[14]
Coals, sawdust, rice straw, and corn stalk	1750 - 1250					[15]
Palm kernel shell (PKS) from palm oil	4000 - 3400		H_2O	O-H	Stretching	[50].
Straw with absorbed glycerol	4000 - 3600					[48]
Solid waste, paper mill sludge, and their blends	4000 - 3500					[49]
Spruce and pine biomass	3900 - 3200	3853, 3568				[35]
Rice straw, sewage sludge, and their blend	1900 - 1600	1750, 1720		C-O(H)		This study
Wood, plastic, tire, and RDF	1900 - 1600					[14]
Spruce and pine biomass	1845 - 1500	1768, 1745	CH_3COOH			[35]
Coals, sawdust, rice straw, and corn stalk	1900 - 1603			C=O	Stretching	[15]
Palm kernel shell (PKS) from palm oil	1900 - 1650					[50]
Solid waste, paper mill sludge, and their blends	1850 - 1600					Fang et al.
Rice straw, sewage sludge, and their blend	1200 - 1100	1120				This study
Wood, plastic, tire, and RDF		1400, 1745	HCOOH	C-O(H)	Stretching	[14]
Coals, sawdust, rice straw, and corn stalk	1200 - 1100					[15]
Rice straw, sewage sludge, and their blend	1400 - 1200	1320. 1250				This study
Wood, plastic, tire, and RDF		1100, 1300				[14]
Spruce and pine biomass	1500 - 1325	1373	C_6H_5OH (Phenol)	O-H	Bending	[35]
Coals, sawdust, rice straw, and corn stalk	1400 - 1200					[15]
Palm kernel shell (PKS) from palm oil	1300 - 1200			C-O	stretching	[50]
Rice straw, sewage sludge, and their blend	1279 - 1100	1100		O-H	Blending	This study
Wood, plastic, tire, and RDF	3000 - 2900					[14]
Spruce and pine biomass	1300 - 950	1165, 1120	CH_3OH (Methanol)			[35]
Palm kernel shell (PKS) from palm oil	1200 - 1000			C-O	Stretching	[50]
Straw with absorbed glycerol	1130 - 1030	1055				[48]
Rice straw, sewage sludge, and their blend	1600 - 1450	1470		C-H	Bending	This study
Spruce and pine biomass	1000 - 650	669, 642	Aromatic			[35]
Palm kernel shell (PKS) from palm oil	1690 - 1450			C=C	Stretching	[50]
Marine sediment	1600 - 1420					[16]
Solid waste, paper mill sludge, and their blends	1850 - 1600					[49]
Straw with absorbed glycerol		1720	Aldehyde	C=O	Stretching	[48]
Marine sediment	1700 - 1600					
Palm kernel shell (PKS) from palm oil	1460 - 1365		Alkanes	C-C; C-H	Stretching	[50]
Marine sediment	850 - 736		NH_3			[16]

RDF: Refuse-derived fuel

435

4. Conclusions

The co-pyrolysis/gasification characteristics and kinetic analysis with or without sewage sludge, rice straw, and their blends additives under different heating rates using TG-FTIR were studied. The results obtained in this research were given as follows. From the rice straw (RS), sewage sludge (SS), and their blends TG and DTG analysis, it was found that SS is decomposed at a lower temperature than RS. The temperature range of volatile matter devolatilization is broader when the extra RS amount is gradually added. RS has a significant influence on the volatile matter released in co-pyrolysis/gasification. Activation energy calculated using the Arrhenius equation could approximately increase from 48.62-53.07 kJ/mol in a linearly correlating behavior with increasing RS addition. The rice straw and their blends exponential factors were in the pyrolysis condition range of $0.71*10^5$ – $18.6*10^6$ (s^{-1}). TGA-FTIR revealed a series of organic species (the gaseous volatile) containing moisture, CO_2, CO, CH_4, acidic gases, and aromatic compounds. In addition, this study also proved that the RS co-pyrolysis/gasification process imposed a significant impact on gaseous pollutants reduction (CO_2, NO, and SO_2). This is an astounding acknowledgment for the co-thermal treatment of partial oxidation performance for some blends. The main volatile components identified by FTIR were aliphatic chains with double bonds, as well as carbonyl, hydroxyl, and C–H groups in organic compounds. In particular, functional groups and gaseous species contributed to the entire pyrolysis reaction were: C=O stretching (2400-2250 cm^{-1}), C-O stretching (2240-2000 cm^{-1}), C-H stretching (3000-2600 cm^{-1}), O-H (4000-3500 cm^{-1}), and SO_2 (1350-1342 cm^{-1}), HCl (2798-2789 cm^{-1}), NO (1762 cm^{-1}) and NH_3 (850-736 cm^{-1}). The experimental results show that RS controlled at 40 wt.% mixed with 60 wt.% SS was the optimum co-thermal treatment proportion. In summary, by exploiting such information, operators or designers can choose a suitable condition for running pyrolysis/gasification in commercial-scale plant in the future.

Declarations

Availability of data and materials

The datasets supporting the conclusions of this article are included within the article.

Competing interests

The authors declare that they have no significant competing financial, professional, or personal interests.

Funding

The authors would like to express their appreciation and gratitude to the Ministry of Science and Technology (MOST) (Project No. MOST-107-2621-M-008-003) for financially supporting this research.

Author's contributions

The manuscript draft was interpreted and written by Thi Ngoc Lan Thao Ngo. Prof. Kung-Yuh Chiang provided technical support, revised the manuscript, and also supervised the research. All authors read and approved the final manuscript.

Acknowledgments

The authors would like to thanks the Precision Instrument Support Center of National Central University in providing the analysis facilities.

References

[1] Chang SS, Lee WJ, Holsen TM, Li HW, Wang LC, Chang C, Guo P, Emissions of polychlorinated-p-dibenzo dioxin, dibenzofurans (PCDD/Fs) and polybrominated diphenyl ethers (PBDEs) from rice straw biomass burning, Atmos. Environ. 94 (2014) 573-581. https://doi.org/10.1016/j.atmosenv.2014.05.067

[2] Judex JW, Gaiffi M, Burgbacher HC, Gasification of dried sewage sludge: Status of the demonstration and the pilot plant, Waste Manage. 32 (2012) 719-723. https://doi.org/10.1016/j.wasman.2011.12.023

[3] Arena U, Process and technological aspects of municipal solid waste gasification, A review. Waste Manage. 32 (2012) 625-639. https://doi.org/10.1016/j.wasman.2011.09.025

[4] Hlina M, Hrabovsky M, Kavka T, Konrad M, Production of high quality syngas from argon/water plasma gasification of biomass and waste, Waste Manage. 34 (2014) 63-66. https://doi.org/10.1016/j.wasman.2013.09.018

[5] Rong L, Maneerung T, Ng JC, Neoh KG, Bay BH, Tong YW, Dai Y, Wang CH, Co-gasification of sewage sludge and woody biomass in a fixed-bed downdraft gasifier: Toxicity assessment of solid residues, Waste Manage. 36 (2015) 241-255. https://doi.org/10.1016/j.wasma-n.2014.11.026

[6] Hu M, Gao L, Chen Z, Ma C, Zhou Y, Chen J, Ma S, Laghari M, Xiao B, Zhang B, Guo D, Syngas production by catalytic in-situ steam co-gasification of wet sewage sludge and pine sawdust, Energy Convers. Manage. 111 (2016) 409-416. https://doi.org/10.1016/j.enconman.20-15.12.064

[7] Mueller A, Haustein HD, Stoesser P, Kreitzberg T, Kneer R, Kolb T, Gasification kinetics of biomass- and fossil-based fuels: Comparison Study Using Fluidized Bed and Thermogravimetric Analysis, Energ Fuel. 29 (2015) 6717-6723. https://doi.org/10.1021/acs.energyfuels.5b01123

[8] Shen F, Liu J, Dong Y, Gu C, Insights into the effect of chlorine on arsenic release during MSW incineration: An on-line analysis and kinetic study, Waste Manage. 75 (2018) 327-332. https://doi.org/10.1016/j.wasman.2018.01.030

[9] Naranjo RA, Conesa JA, Pedretti EF, Romero OR, Kinetic analysis: Simultaneous modeling of pyrolysis and combustion processes of dichrostachys cinerea, Biomass and Bioenerg. 36 (2012) 170-175. https://doi.org/10.1016/j.biombioe.2011.10.032

510 [10] Yang J, Xu X, Liang S, Guan R, Li H, Chen Y, Liu B, Enhanced hydrogen production in catalytic
511 pyrolysis of sewage sludge by red mud: Thermogravimetric kinetic analysis and pyrolysis
512 characteristics, Int. J. Hydrog. Energy. 43 (2018) 7795-7807. https://doi.org/10.1016/j.ijhydene.
513 2018.03.018
514 [11] Soria-Verdugo A, Goos E, Morato-Godino A, García-Hernando N, RiedelU, Pyrolysis of biofuels
515 of the future: Sewage sludge and microalgae - Thermogravimetric analysis and modelling of the
516 pyrolysis under different temperature conditions, Energy Convers. Manag. 138 (2017) 261-272.
517 https://doi.org/10.1016/j.enconman.2017.01.059
518 [12] Tang Y, Ma X, Lai Z, Yu Q, Oxy-fuel combustion characteristics and kinetics of microalgae and its
519 mixture with rice straw using thermogravimetric analysis. Int. J. Energy Res. 42 (2018) 532-541.
520 https://doi.org/10.1002/er.3836
521 [13] Eskander SB, Tawfik ME, Tawfic ML, Mechanical, flammability and thermal degradation
522 characteristics of rice straw fiber-recycled polystyrene foam hard wood composites incorporating fire
523 retardants, J Therm Anal Calorim. 132 (2018) 1115-1124. https://doi.org/10.1007/s10973-018-69846
524 [14] Singh S, Wu CF, Williams PT, Pyrolysis of waste materials using TGA-MS and TGA-FTIR as
525 complementary characterization techniques, J. Anal. Appl. Pyrol. 107 (2012) 94-99. https://doi.org/
526 10.1016/j.jaap.2011.11.011
527 [15] Xu CF, Hu S, Xiang J, Zhang LQ, Sun LS, Shuai C, Chen QD, He LM, Edreis EMA, Interaction
528 and kinetic analysis for coal and biomass co-gasification by TG–FTIR, Bioresour. Technol. 154
529 (2014) 313-321. https://doi.org/10.1016/j.biortech.2013.11.101
530 [16] Oudghiri F, García-Morales JL, Rodríguez-Barroso MR, Novel use of TGA–FTIR technique to
531 predict the pollution degree in marine sediments, Int. J. Hydrog. Energy. 41 (2016) 8154-8158.
532 [17] Chiang KY, Chien KL, Lu CH, Characterization and comparison of biomass produced from various
533 sources: Suggestions for selection of pretreatment technologies in biomass-to-energy, Appl Energ.
534 100 (2012) 164–171. https://doi.org/10.1016/j.apenergy.2012.06.063
535 [18] Reyes-Labarta JA, Marcilla A, Kinetic study of the decompositions involved in the thermal
536 degradation of commercial azodicarbonamide, J. Appl. Polym. Sci. 107 (2008) 339-346.
537 https://doi.org/10.1002/app.26922

538 [19] Bakar RA, Yahya R, Production of High Purity Amorphous Silica from Rice Husk, Procedia Chem.
539 19 (2016) 189-195. https://doi.org/10.1016/j.proche.2016.03.092
540 [20] Mansaray KG, Ghaly AE, Determination of Reaction Kinetics of Rice Husks in Air Using
541 Thermogravimetric Analysis, Energ Source. 21 (1999) 899-911.
542 [21] Lee T, Zubir ZA, Jamil FM, Matsumoto A, Yeoh FY, Combustion and pyrolysis of activated carbon
543 fibre from oil palm empty fruit bunch fibre assisted through chemical activation with acid treatment,
544 J Anal Appl Pyrol. 110 (2014) 408-418. https://doi.org/10.1016/j.jaap.2014.10.010
545 [22] Bartocci P, Anca-Couce A, Slopiecka K, Nefkens S, Evic N, Retschitzegger S, Barbanera M, Buratti
546 C, Cotana F, Bidini G, Fantozzi F, Pyrolysis of pellets made with biomass and glycerol: Kinetic
547 analysis and evolved gas analysis, Biomass Bioenerg. 97 (2017) 11-19. https://doi.org/10.1016/
548 j.biombioe.2016.12.004
549 [23] Lin YS, Ma XQ, Ning XX, Yu ZS, TGA–FTIR analysis of co-combustion characteristics of paper
550 sludge and oil-palm solid wastes, Energy Conversion and Management. 89 (2015) 727-734.
551 [24] Branca C, Di Blasi C, Global Kinetics of Wood Char Devolatilization and Combustion, Energ Fuel.
552 17 (2003) 1609-1615. https://doi.org/10.1021/ef030033a
553 [25] Ahuja P, Singh PC, Upadhyay S, Kumar S, Kinetics of biomass and sewage sludge pyrolysis:
554 Thermogravimetric and sealed reactor studies, Indian J. Chem. Technol. 3 (1996) 306-312.
555 [26] Bungay VC, Kinetic study on pyrolysis and gasification of plastic waste, Chem. Eng. Trans. 56
556 (2017) 193-198. https://doi.org/10.3303/CET1756033
557 [27] Özsin G, Pütün AE, Kinetics and evolved gas analysis for pyrolysis of food processing wastes using
558 TGA/MS/FT-IR, Waste Manage. 64 (2017) 315-326. https://doi.org/10.1016/j.wasm-an.2017.03.020
559 [28] Zhang SQ, Yue XM, Yin ZY, Pan TT, Dong MJ, Sun TY, Study of the co-pyrolysis behavior of
560 sewage-sludge/rice-straw and the kinetics, Procedia Earth Planet Sc. 1 (2009) 661-666.
561 https://doi.org/10.1016/j.proeps.2009.09.104
562 [29] Shao JG, Yan R, Chen HP, Wang BW, Lee DH, Liang DT, Pyrolysis characteristics and kinetics of
563 sewage sludge by thermogravimetry fourier transform infrared analysis, Energ Fuel. 22 (2008) 38-
564 45. https://doi.org/10.1021/ef700287p

565 [30] Piatkowski N, Steinfeld A, Reaction kinetics of the combined pyrolysis and steam-gasification of
566 carbonaceous waste materials, Fuel. 89 (2010) 1133-1140. https://doi.org/10.1016/ j.fuel.2009-
567 .11.011
568 [31] Wang S, Wang Q, Hu YM, Xu SN, He ZX, Ji HS, Study on the synergistic co-pyrolysis behaviors
569 of mixed rice husk and two types of seaweed by a combined TG-FTIR technique, J Anal Appl Pyrol.
570 114 (2015) 109-118. https://doi.org/10.1016/j.jaap.2015.05.008
571 [32] Parthasarathy P, Narayanan KS, Arockiam L, Study on kinetic parameters of different biomass
572 samples using thermo-gravimetric analysis, Biomass Bioenerg. 58 (2013) 58-66. https://doi.org/
573 10.1016/j.biombioe.2013.08.004
574 [33] El-Sayed SA, Mostafa ME, Kinetic Parameters Determination of Biomass Pyrolysis Fuels Using
575 TGA and DTA Techniques, Waste Biomass Valori. 6 (2015) 401-415. https://doi.org/10.1007/
576 s12649-015-9354-7
577 [34] Raheem A, Dupont V, Channa AO, Zhao X, Vuppaladadiyam AK, Taufiq-Yap YH, Zhao M, Harun
578 R, Parametric Characterization of Air Gasification of Chlorella vulgaris Biomass, Energ Fuel. 31
579 (2017) 2959-2969. https://doi.org/10.1021/acs.energyfuels.6b03468
580 [35] Salema AA, Afzal MT, Motasemi F, Is there synergy between carbonaceous material and biomass
581 during conventional pyrolysis? A TG-FTIR approach, J Anal Appl Pyrol. 105 (2014) 217-226.
582 https://doi.org/10.1016/j.jaap.2013.11.007
583 [36] Wang GW, Zhang JL, Shao JG, Sun H, Zuo HB, Thermogravimetric Analysis of Coal Char
584 Combustion Kinetics, J Iron Steel Res Int. 21 (2014) 897-904. https://doi.org/10.1016/
585 S1006706X(14)60159-X
586 [37] Zeng X, Wang F, Wang YG, Li AM, Yu J, Xu GW, Characterization of Char Gasification in a Micro
587 Fluidized Bed Reaction Analyzer, Energ Fuel. 28 (2014) 1838-1845. https://doi.org/10.1016/
588 j.fuproc.2015.04.025
589 [38] Jayaraman K, Kok MV, Gokalp I, Pyrolysis, combustion and gasification studies of different sized
590 coal particles using TGA-MS, Appl. Therm. Eng. 125 (2017) 1446-1455. https://doi.org/
591 10.1016/j.applthermaleng.2017.07.128

592 [39] Cai J, Wang Y, Zhou L, Huang Q, Thermogravimetric analysis and kinetics of coal/plastic blends
593 during co-pyrolysis in nitrogen atmosphere, Fuel Process. Technol. 89 (2008) 21-27. https://doi.org/
594 10.1016/j.fuproc.2007.06.006
595 [40] Brittain HG, Bruce RD, Chapter 4: Thermal analysis. Comprehensive Analytical Chemistry,
596 Elsevier. 47 (2006) 63-109. https://doi.org/10.1016/j.fuproc.2007.06.006
597 [41] Chen W, Annamalai K, Sun JF, Chen YM, Chemical kinetics of bean straw biofuel pyrolysis using
598 maximum volatile release method. Korean J Chem Eng. 33 (2016) 2330-2336.
599 https://doi.org/10.1007/s11814-016-0088-4
600 [42] Sun Z, Chen S, Russell CK, Hu J, Rony AH, Tan G, Chen A, Duan L, Boman J, Tang J, Chien T,
601 Fan M, Xiang W, Improvement of H_2-rich gas production with tar abatement from pine wood
602 conversion over bi-functional $Ca_2Fe_2O_5$ catalyst: Investigation of inner-looping redox reaction and
603 promoting mechanisms, Appl Energ. 212 (2018) 931-943. https://doi.org/10-.1016/ j.apenergy.
604 2017.12.087
605 [43] Mopoung S, Moonsri P, Palas W, Khumpai S, Characterization and Properties of Activated Carbon
606 Prepared from Tamarind Seeds by KOH Activation for Fe(III) Adsorption from Aqueous Solution,
607 Sci. World J. 415961 (2015) 9 pages. https://doi.org/10.1155/2015/415961
608 [44] Vasile C, Brebu MA, Thermal valorization of biomass and of synthetic polymer waste. Upgrading
609 of pyrolysis oils, Cell Chem Technol. 40 (2007) 489-512.
610 [45] Zhou L, Zhang G, Reinmöller M, Meyer B, Effect of inherent mineral matter on the co-pyrolysis of
611 highly reactive brown coal and wheat straw, Fuel. 239 (2019) 1194-1203. https://doi.org/
612 10.1016/j.fuel.2018.11.114
613 [46] Zhang X, Lei H, Zhu L, Zhu X, Qian M, Yadavalli G, Wu J, Chen S, Thermal behavior and kinetic
614 study for catalytic co-pyrolysis of biomass with plastics, Bioresour. Technol. 220 (2016) 233-238.
615 https://doi.org/10.1016/j.biortech.2016.08.068
616 [47] Wu Z, Li Y, Zhang B, Yang W, Yang B, Co-pyrolysis behavior of microalgae biomass and low-rank
617 coal: Kinetic analysis of the main volatile products, Bioresour. Technol. 271 (2019) 202-209.
618 https://doi.org/10.1016/j.biortech.2018.09.076

[48] Striūgas N, Skvorčinskienė R, Paulauskas R, Zakarauskas K, Vorotinskienė L, Evaluation of straw with absorbed glycerol thermal degradation during pyrolysis and combustion by TG-FTIR and TG-GC/MS, Fuel. 204 (2017) 227-235. https://doi.org/10.1016/j.fuel.2017.05.063

[49] Fang SW, Yu ZS, Lin Y, Lin YS, Fan YL, Liao YF, Ma XQ, A study on experimental characteristic of co-pyrolysis of municipal solid waste and paper mill sludge with additives, Appl Therm Eng. 111 (2017) 292-300. https://doi.org/10.1016/j.applthermaleng.2016.09.102

[50] Ma ZQ, Chen DY, Gu J, Bao BF, Zhang QS, Determination of pyrolysis characteristics and kinetics of palm kernel shell using TGA–FTIR and model-free integral methods, Energy Convers. Manag. 89 (2015) 251-259. https://doi.org/10.1016/j.enconman.2014.09.074

[51] Blázquez G, Pérez A, Iáñez-Rodríguez I, Martínez-García C, Calero M, Study of the kinetic parameters of thermal and oxidative degradation of various residual materials, Biomass Bioenerg. 124 (2019) 13-24. https://doi.org/10.1016/j.biombioe.2019.03.008

[52] Parshetti GK, Quek A, Betha R, Balasubramanian R, TGA–FTIR investigation of co-combustion characteristics of blends of hydrothermally carbonized oil palm biomass (EFB) and coal, Fuel Process Technol.118 (2014) 228-234. https://doi.org/10.1016/j.fuproc.2013.09.010

[53] Stephen JL, Periyasamy B, Innovative developments in biofuels production from organic waste materials: A review, Fuel. 214 (2018) 623-633. https://doi.org/10.1016/j.fuel.2017.11.042

[54] Antti L, Leonid K, Mika P, Markku R, Large blue shift of the H–Kr stretching frequency of HKrCl upon complexation with N_2, J. Chem. Phys. 117 (2002) 961-964. https://doi.org/10.1063/1-.1491403

[55] Jiang LB, Yuan XZ, Li H, Chen XH, Xiao ZH, Liang J, Leng LJ, Guo Z, Zeng GM, Co-pelletization of sewage sludge and biomass: Thermogravimetric analysis and ash deposits, Fuel Process Technol. 145 (2016) 109-115. https://doi.org/10.1016/j.fuproc.2016.01.027

Figures

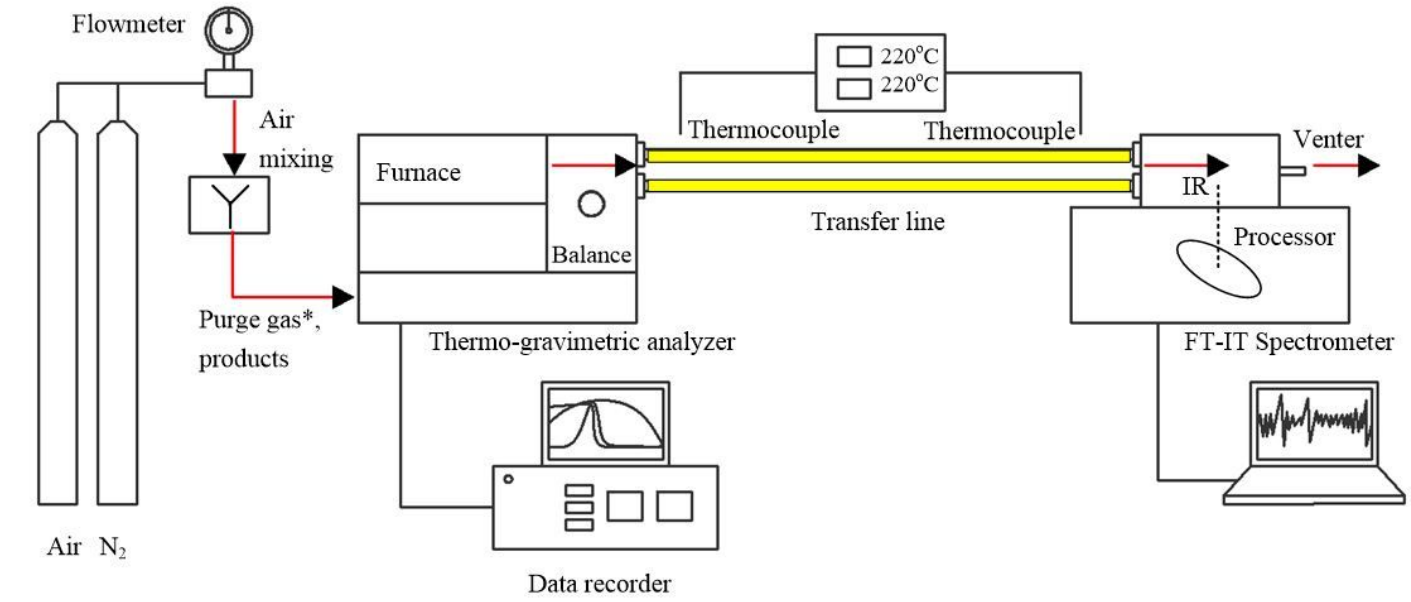

Note the purge gas* used were nitrogen and air for TGA and TGA-FTIR, respectively.

Figure 1

Schematic diagram of TGA-FTIR experiment

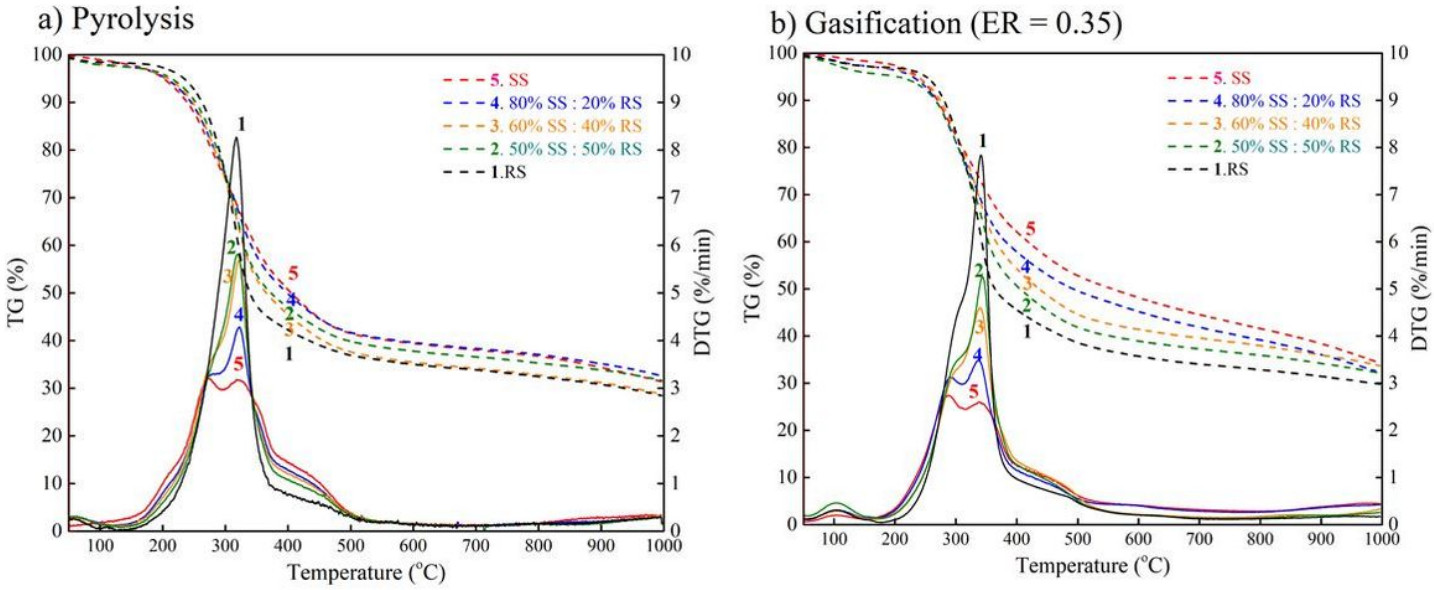

Figure 2

A comparison between TG/DTG curves detected from rice straw, sewage sludge and their additives pyrolysis and air gasification at 10 oC/min heating rate

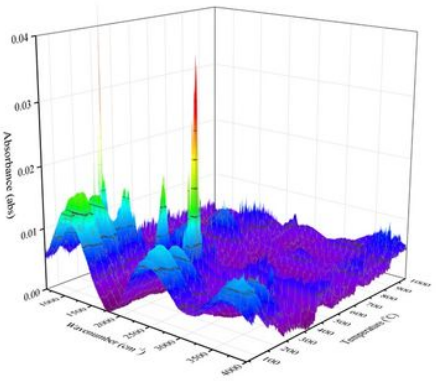

a) 3D FTIR diagram of rice straw

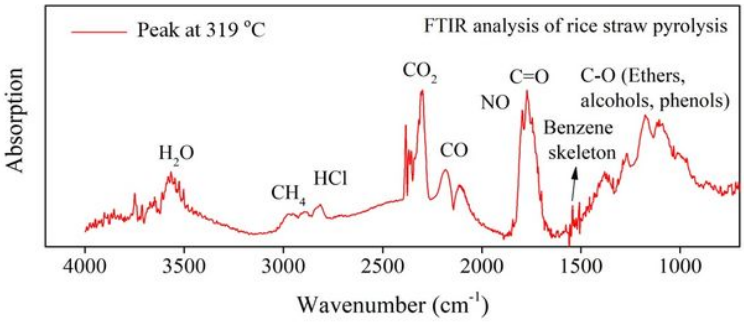

b) FTIR spectrum for volatiles in rice straw pyrolysis

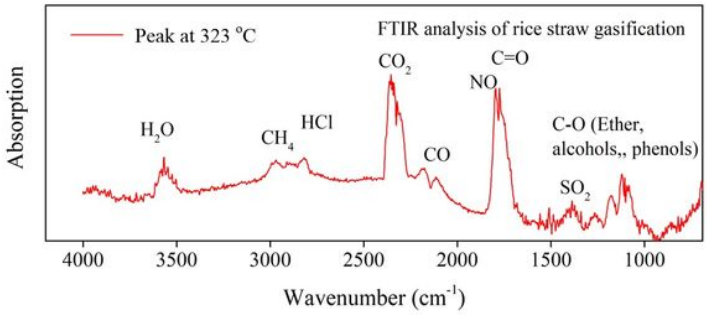

c) FTIR spectrum for volatiles in rice straw gasification

Figure 3

FTIR analysis of rice straw pyrolysis/gasification with a heating rate of 10 oC/min

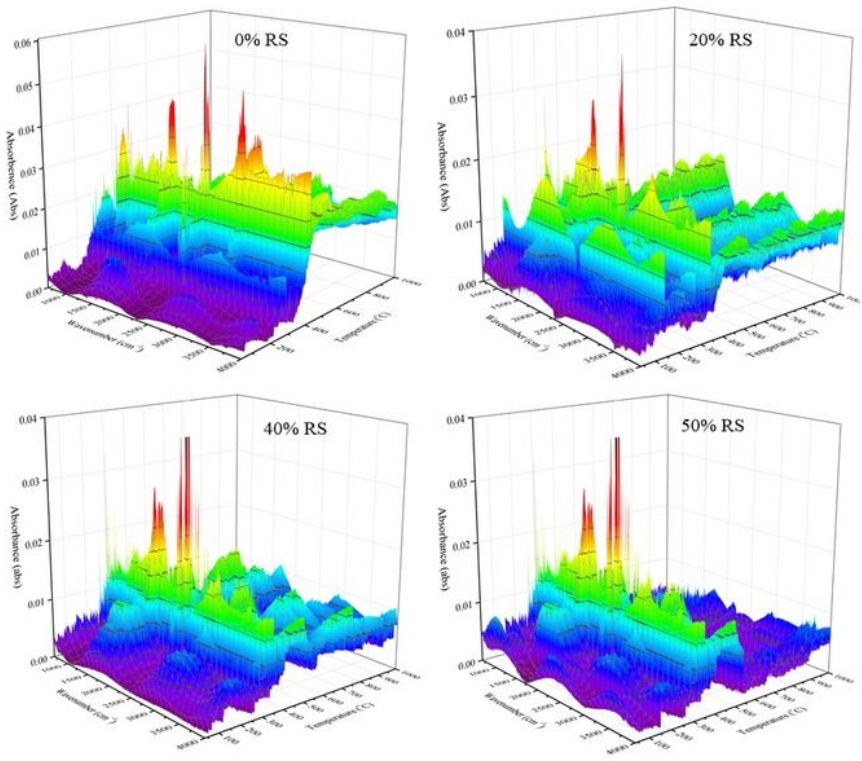

a) 3D FTIR diagrams

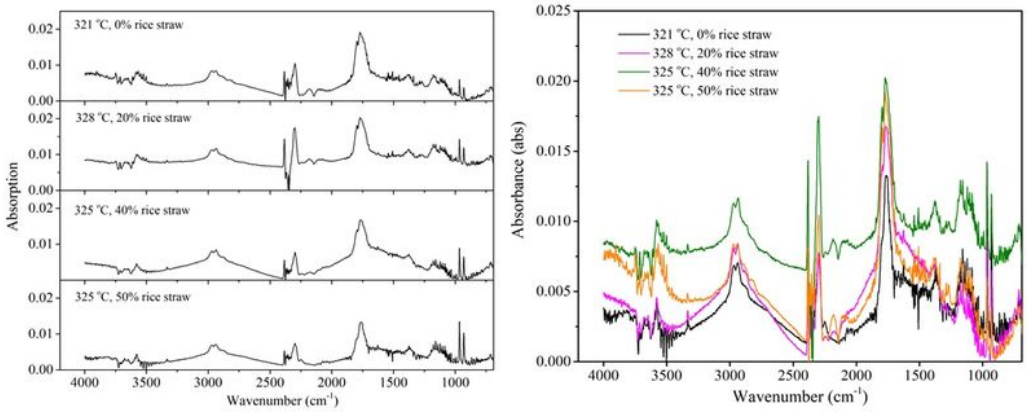

b) FTIR absorption spectra of products evolved during co-pyrolysis.

Figure 4

Gas released from sewage sludge, and their mixtures with rice straw as detected by TGA-FTIR